



# Fluorescent cyanine-guanidiniocarbonyl-pyrrole conjugate with pH-dependent DNA/RNA recognition and DPP III fluorescent labelling and inhibition properties

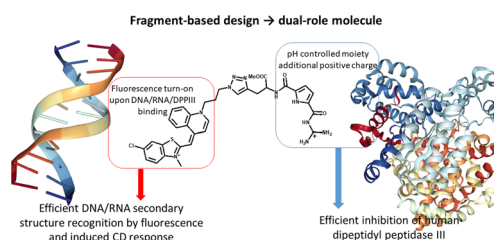
Tamara Šmidlehner<sup>1</sup> · Zrinka Karačić<sup>1</sup> · Sanja Tomić<sup>1</sup> · Carsten Schmuck<sup>2</sup> · Ivo Piantanida<sup>1</sup>

Received: 28 February 2018 / Accepted: 18 March 2018  
© Springer-Verlag GmbH Austria, part of Springer Nature 2018

## Abstract

Here designed and prepared cyanine-guanidiniocarbonyl-pyrrole conjugate (Cy-GCP), intrinsically non-fluorescent, revealed fluorescent switch-on recognition of various secondary structures of ds-DNA and ds-RNA. Moreover, at the same submicromolar concentrations, DNA/RNA recognition was observed by selective induced (I)CD pattern in the visible range. Preliminary results showed that Cy-GCP strongly interacted with DPP III enzyme, switching-on the fluorescence upon binding and inhibiting enzyme action with efficiency comparable to the best-known inhibitor tyrnorphin.

## Graphical abstract



**Keywords** DNA/RNA recognition · Circular dichroism · Fluorescence · DPP III enzyme binding · DPP III inhibition

## Introduction

The fragment-based design combines structures with properties of interest into one molecule, which shows enhanced properties of each component. This approach is widely used in drug discovery to obtain more potent drugs or biomolecular tools and probes [1].

**Electronic supplementary material** The online version of this article (<https://doi.org/10.1007/s00706-018-2192-0>) contains supplementary material, which is available to authorized users.

✉ Tamara Šmidlehner  
tsmidleh@irb.hr

<sup>1</sup> Ruđer Bošković Institute, Zagreb, Croatia

<sup>2</sup> Institute for Organic Chemistry, University of Duisburg-Essen, Essen, Germany

Cyanine dyes (Cy) are known as intrinsically non-fluorescent but with intense fluorescence emission switched-on upon binding to a target (e.g. DNA, RNA, proteins) as a result of restricted rotation around methine bridge [2, 3]. Our previous research showed that cyanine dyes are capable of recognising between similar secondary structures of various DNA or RNA by a combination of two mutually independent, highly sensitive and selective spectroscopic methods: fluorescence emission and binding-induced circular dichroism [4–6].

One of the essential naturally occurring amino acids, arginine, bases all its biological functions on interactions of positively charged guanidine unit incorporated in its side chain. This initiated the question whether guanidinium analogue with the ability to adjust protonation to the biological environment would also allow tuning of the interactions with various biological targets, as DNA, RNA

or proteins. Indeed, due to the guanidine protonation ( $pK$  5.5), the guanidiniocarbonyl-pyrrole moiety (GCP) showed pH-controllable interactions with nucleic acids [7, 8] and demonstrated also highly effective enzyme inhibition such as cysteine protease [9].

In this context, the recent results on a small molecule consisting of fluorophore (pyrene) and GCP unit draw our attention, since the same small molecule (Scheme 1, Py-GCP) acted as dual probe: selective and pH-controllable DNA/RNA binder [8], as well as the efficient human dipeptidyl peptidase III (hDDP III) probe and inhibitor [10]. The dipeptidyl peptidases III (DDP III) are quite ubiquitous zinc-exopeptidases cleaving dipeptides from the N-termini of its oligopeptide substrates, particularly interesting because their exact biological role is unknown—therefore, the development of fluorescent inhibitor could allow monitoring of DDP III *in vitro* or *in vivo* action [11].

Herein, we applied fragment-based design approach and coupled cyanine dye with a guanidiniocarbonyl-pyrrole moiety to yield molecule Cy-GCP (Scheme 1) with pH-regulated net charge of 1+ at pH 7 or 2+ at pH 5, which should preferably have a double role: DNA/RNA recognition and inhibition of dipeptidyl peptidase III (DPP III).

## Results and discussion

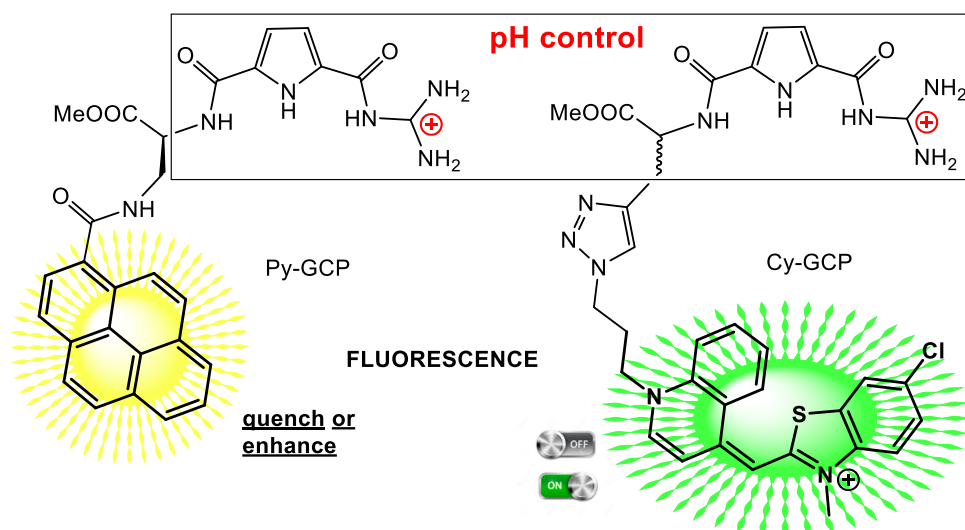
### Physicochemical properties of Cy-GCP

The physicochemical properties of the novel conjugate Cy-GCP were investigated at physiological pH 7 and at pH 5 due to known pH sensitivity of guanidiniocarbonyl-pyrrole

(GCP) moiety [8]. Cy-GCP is stable in aqueous media at both pH overnight, i.e. no pronounced change in absorption was observed (ESI, Fig. S1). The UV–Vis spectra of Cy-GCP at both pH (Fig. 1) revealed two pronounced absorption regions, one ( $\lambda_{\max}$  around 300 nm) originating from overlapped absorbancies of guanidiniocarbonyl-pyrrole and triazole (incorporated in the linker) moieties and another absorption band in the visible range attributed to cyanine dye ( $\lambda_{\max} = 480\text{--}510$  nm). Both absorbancies were linearly dependent on concentration at micromolar conditions, allowing determinations of molar extinction coefficients (Table 1).

The GCP pH-dependent protonation had almost negligible influence on the GCP absorbance (absorbance measured at pH 5 and pH 7 are shown in Fig. 1,  $\lambda_{\max} = 297$  nm), while surprisingly pronounced differences were observed in cyanine absorption region (450–550 nm). Namely, at pH 7 two bands were observed in this region, with slightly dominant one at 480 nm, while at pH 5 only the band at 510 nm was found. According to the literature, 510 nm band could be attributed to single cyanine chromophore, while blue-shifted maximum at 480 nm corresponds to the H-type cyanine aggregate formation [2, 12]. Similarly to the previously reported results, dissociation of the aggregate with temperature increase was noticed (ESI, Fig. S1) [4–6]. At pH 5, the aggregation of cyanine is disfavoured, most likely because the repulsive interactions between the protonated guanidiniocarbonyl-pyrrole moieties hamper the efficient aromatic stacking (necessary for aggregation). Cy-GCP has negligible fluorescence emission and very weak CD spectrum at studied conditions (data not shown).

Scheme 1



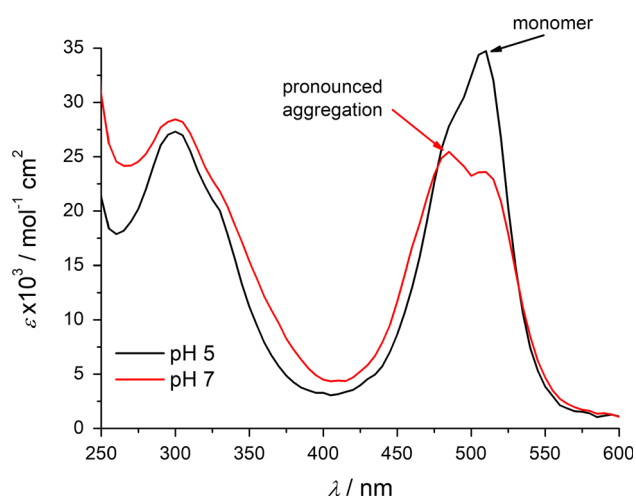


**Fig. 1** UV-Vis spectra of Cy-GCP ( $c = 1.6 \times 10^{-6} \text{ mol dm}^{-3}$ ) at pH 5 (black line) and at pH 7 (red line) (colour figure online)

**Table 1** Molar extinction coefficients ( $\epsilon$ ) at a wavelength of maximum Cy-GCP absorption at different pH

pH	Absorption moiety	$\lambda/\text{nm}$	$\epsilon/\text{mol}^{-1} \text{ cm}^2$
5	GCP	297	27,304
	Cy	510	34,535
7	GCP	297	28,430
	Cy	510	24,074

### Study of the Cy-GCP interactions with DNA/RNA

Due to pronounced aggregation of the Cy-GCP at micromolar concentrations, UV-Vis titrations were not suitable for determination of interactions with DNA/RNA. However, the exceptionally strong fluorescence of cyanine dye upon binding to DNA allowed fluorimetric titrations at  $0.1 \mu\text{M}$  concentration of Cy-GCP, at which aggregation is negligible.

Upon addition of any ds-DNA or ds-RNA and excitation of cyanine moiety at 510 nm, an intense cyanine fluorescence was observed at 530 nm for ds-DNAs and at 537 nm for AU-RNA (Fig. 2). Processing of titration data by Scatchard equation [13, 14] resulted with the binding constant and related parameters (Table 2). According to the data obtained, Cy-GCP showed similar, micromolar affinity towards all analysed nucleic acids. The only exception was the order of magnitude stronger binding of Cy-GCP to GC-DNA at pH 7.

At both pH, Cy-GCP showed clear tendency in emission intensity response following  $\text{Int(AT-DNA)} \ll \text{Int(ctDNA: 48\% GC)} = \text{Int(GC-DNA)}$ , which strongly supported emission selectivity of Cy-GCP toward GC-DNA sequences.

Intriguingly, AU-RNA induced three times stronger emission intensity than AT-DNA (Table 2; Fig. 2). Although these polynucleotides consist of almost identical basepairs, they differ strongly in secondary structure. Namely, AT-DNA is typical B-helix, while AU-RNA has A-helical structure [16].

Furthermore, to get better insight into the binding mode of Cy-GCP to polynucleotides, circular dichroism titrations were performed [17]. This method can report changes of polynucleotide conformation upon ligand binding while the orientation of the induced CD signal in the region, where only ligand absorbs light ( $> 300 \text{ nm}$ ), gives information about the relative geometry of formed ligand/polynucleotide complex [18]. Due to the strong CD spectrum of polynucleotides, it was not possible to unambiguously discuss the changes in CD spectra at wavelengths below 300 nm. However, both Cy-GCP chromophores, GCP and Cy, absorb in spectrum region above 300 nm, in 300–330 nm and in 540–550 nm range, respectively, thus allowing detection of induced (ICD) bands eventually occurring upon DNA/RNA binding. Convenient separation between Cy and GCP spectral range allowed separate monitoring of chromophores. Furthermore, due to the tendency of Cy-GCP to aggregate, its concentrations upon adding to polynucleotide were kept as low as possible, starting from  $0.2 \mu\text{M}$  up till  $1.6 \mu\text{M}$  concentration.

In all performed experiments strong positive ICD bands appeared in Cy-range (Fig. 3, 450–550 nm), thus excluding intercalation into DNA (which should give weak negative ICD) [18]. Detailed analysis revealed similar ICD response for all DNAs, whereby at large excess of DNA over dye ( $r_{[\text{Cy-GCP}]/[\text{polynucleotide}]} = 0.01; 0.02$ ) positive ICD suggested minor groove binding, followed by bisignate ICD at  $r > 0.02$  characteristic for Cy-aggregation within the DNA groove [3, 16]. Intriguingly, AU-RNA induced (ICD) band was significantly blue-shifted in comparison with the one induced by DNA and, moreover, it showed pH dependence: at neutral conditions (Fig. 3b), only positive ICD band characteristic for single Cy-chromophore positioned most likely in RNA major groove was present, whereas at pH 5 no ICD was observed till the highest ratio  $r = 0.08$ , at which bisignate ICD of Cy-aggregate appeared (Fig. 3a).

Changes in the 300–330 nm CD spectrum range are attributed to the binding of guanidiniocarbonyl-pyrrole of Cy-GCP to polynucleotide double helix, whereby ICD bands strongly depend on the pH media due to the aforementioned protonation of GCP [7]. At neutral pH, the ICD bands were in general of lower intensity, and only those for AT-DNA were of a positive sign (typical for minor groove binding), while AU-RNA and GC-DNA yielded negative ICD likely due to the poorly defined minor groove. At pH 5, the positive ICD band for AT-DNA remained but GC-DNA yielded now positive ICD, strongly bathochromically

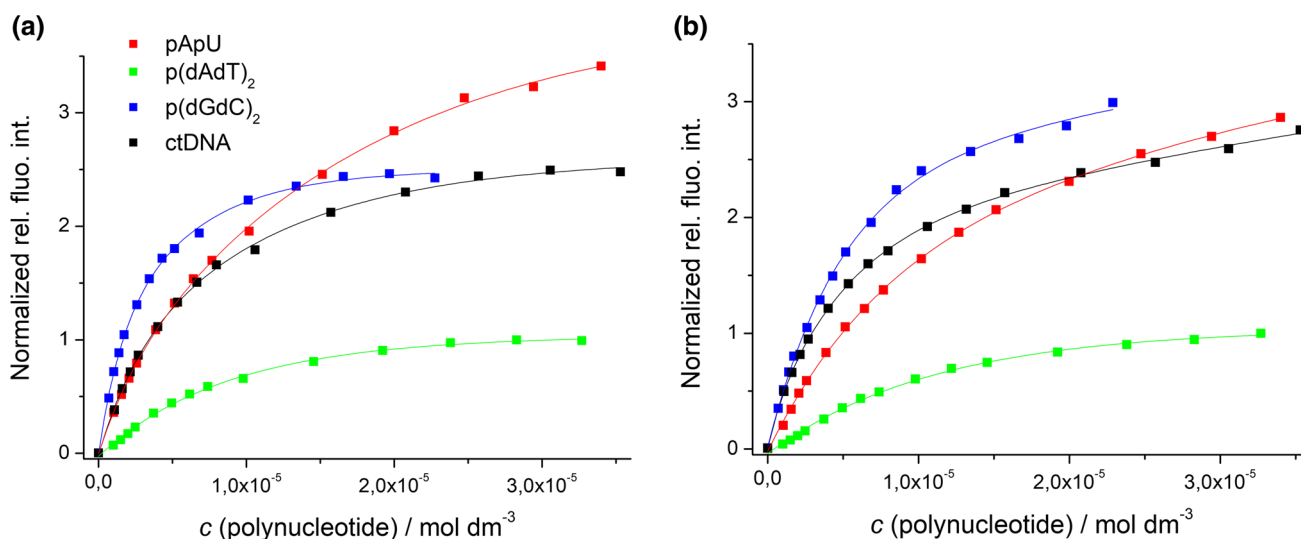


**Fig. 2** The increase of Cy-GCP fluorescence ( $\lambda_{\text{exc}} = 510 \text{ nm}$ ,  $c = 1 \times 10^{-7} \text{ mol dm}^{-3}$ ) upon addition of polynucleotides at: **a** pH 7; **b** pH 5. Data were normalised to the final intensity of AT-DNA titration to visualise the emission selectivity

**Table 2** Binding constants ( $\log K_s$ )<sup>a</sup> and quantum yields ( $QY$ )<sup>b</sup> of the Cy-GCP/ds-polynucleotides complexes calculated by processing fluorimetric titrations ( $c(\text{Cy-GCP}) = 1 \times 10^{-7} \text{ mol dm}^{-3}$ ), sodium cacodylate buffer,  $I = 0.05 \text{ mol dm}^{-3}$

pH		ctDNA	p(dAdT) <sub>2</sub>	p(dGdC) <sub>2</sub>	pApU
5	$\log K_s$	6.4	5.9	6.5	5.9
	$QY$	0.013	0.005	0.013	0.019
7	$\log K_s$	6.4	6.1	7.3	5.9
	$QY$	0.011	0.004	0.015	0.014

<sup>a</sup>Processing of titration data by means of Scatchard equation [13, 14] gave values of ratio  $n[\text{bound Cy-GCP}]/[\text{polynucleotide}] = 0.1\text{--}0.3$ , for easier comparison all  $\log K_s$  values were re-calculated for fixed  $n = 0.1$ . Correlation coefficients were  $> 0.99$  for all calculated  $K_s$

<sup>b</sup> $QY$  was determined with respect to the rhodamine 6G standard ( $QY = 0.95$ ) [15]

shifted in comparison to AT-DNA. Such strong red shift can be attributed to difference in minor groove environment, in which GC-DNA has protruding amino groups of guanine severely limiting the insertion of GCP. Intriguingly AU-RNA did not yield any ICD at pH 5 that can be attributed to GCP binding, thus suggesting heterogeneous orientation of GCP moiety with respect to helix chiral axis.

The thermal denaturation experiments of ds-polynucleotides with small molecules provide information about the influence of ligand on the ds-helix stability [19, 20]. The impact of Cy-GCP conjugate on stabilisation of ds-polynucleotides is stronger at pH 5 than at pH 7 (Table 3), which can be attributed to protonation of GCP and its electrostatic interactions with the negatively charged DNA/RNA backbone. The more pronounced stabilisation of AT-DNA with respect to AU-RNA or GC-DNA is consistent with CD results, showing better positioning of GCP unit

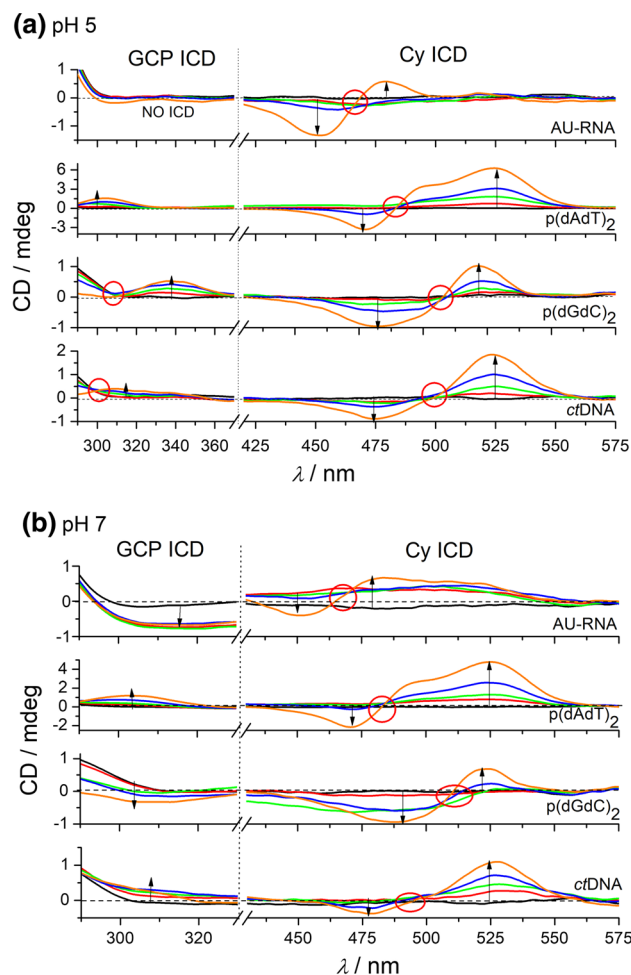


**Fig. 3** ICD spectra of Cy-GCP with different polynucleotides ( $c = 2 \times 10^{-5} \text{ mol dm}^{-3}$ , black lines) at: **a** pH 5; **b** pH 7. Red circles show isodichroic points,  $r_{[\text{Cy-GCP}]/[\text{polynucleotide}]} = 0.01$  (red); 0.02 (green); 0.04 (blue); 0.08 (orange) (colour figure online)

**Table 3**  $\Delta T_m$  values ( $^{\circ}\text{C}$ ) for different ratios  $r$  of Cy-GCP added to the polynucleotide

$r$	ctDNA		p(dAdT) <sub>2</sub>		pApU	
	pH 5	pH 7	pH 5	pH 7	pH 5	pH 7
0.02	1.7	0	2.5	2.1	2.3; <sup>a</sup> 0	1.1
0.04	1.7	0	5.9	3.6	2.3; <sup>a</sup> 0	1.1
0.06	5.5	2.5	11.5	6.0	3.3; <sup>a</sup> 0	2.2

Error in  $\Delta T_m \pm 0.5$   $^{\circ}\text{C}$

$r = [\text{compound}]/[\text{polynucleotide}]$

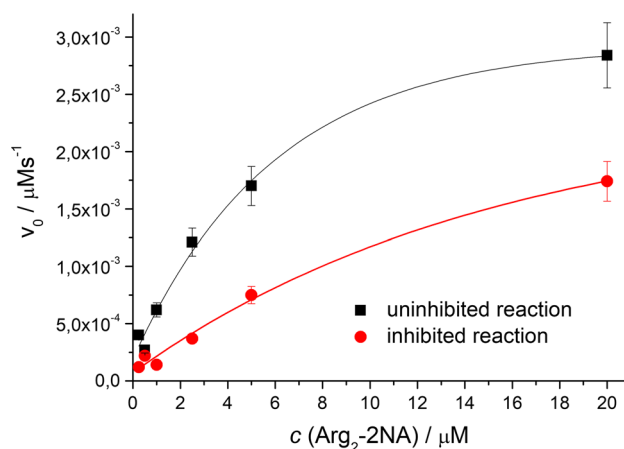
<sup>a</sup>Biphasic transitions: the first transition at  $T_m$  28.5  $^{\circ}\text{C}$  is attributed to denaturation of polyA–polyU and the second transition at  $T_m$  80.1  $^{\circ}\text{C}$  is attributed to denaturation of polyAH<sup>+</sup>–polyAH<sup>+</sup> since poly A at pH 5 is mostly protonated and forms ds-polynucleotide [14, 18]

within AT-DNA minor groove with respect to grooves containing GC-basepairs or poorly defined AU-RNA groove [14].

### Interactions of Cy-GCP with DPP III enzyme

The Cy-GCP could interact with DPP III either as a substrate (since it is dipeptide as well) or as an inhibitor, whereby for both actions strong binding to enzyme is essential. Thus, to assess the binding affinity of Cy-GCP toward DPP III avoiding eventual Cy-GCP enzymatic disintegration we performed fluorimetric titration with DPP III mutant with abolished enzymatic activity (E451A). Processing of titration data (ESI, Fig. S10) yielded moderate binding constant  $\log K_s = 5$ , comparable to the previously determined affinity of pyrene-, or phenanthridine-GCP analogues [10]. Further experiments with Cy-GCP and enzymatically active (wt) DPP III revealed no change in spectral properties of Cy-GCP in commonly studied time range, thus excluding Cy-GCP as an enzyme–substrate.

To test the potential inhibitory activity of the Cy-GCP, the reaction of human DPP III with an artificial substrate Arg<sub>2</sub>-2NA in the presence of Cy-GCP was monitored fluorimetrically by detecting the release of product 2-naphthylamine ( $\lambda_{\text{exc}} = 332$  nm,  $\lambda_{\text{em}} = 420$  nm). The Cy-GCP showed inhibition of DPP III as a mixed type inhibitor (Fig. 4), with the largest effect on the Michaelis constant ( $K_M$ ): in the inhibited reaction, it was increased approximately three times (Table 4). The inhibition constant  $K_I$  is 73 nM, indicating that Cy-GCP is as effective DPP III inhibitor as peptide tynorphin (70 nM) [21] and it is the order of magnitude more effective in comparison to synthetic small molecule analogues studied previously [10].

**Fig. 4** Reaction profile of uninhibited reaction of DPP III with Arg<sub>2</sub>-2NA as substrate and with the addition of Cy-GCP (0.2  $\mu\text{M}$ ), in 20 mM Tris-HCl buffer pH 7.4**Table 4** Kinetic parameters for DPP III inhibition with Cy-GCP

Reaction	Uninhibited	Inhibited (0.2 $\mu\text{M}$ Cy-GCP)
$K_M/\mu\text{M}$	$5.0 \pm 0.7$	$16 \pm 3$
$V_{\text{max}}/\mu\text{M s}^{-1}$	$0.00356 \pm 0.00019$	$0.00315 \pm 0.00035$
$k_{\text{cat}}/\text{s}^{-1}$	$36 \pm 2$	$31 \pm 4$

### Conclusion

Here, we presented a novel cyanine-guanidiniocarbonyl-pyrrole (Cy-GCP) conjugate with a dual role, showing pH controlled fluorescence and ICD recognition of ds-DNA/RNA by minor/major groove binding and also targeting particular enzyme—showing DPP III inhibitory activity.

Comparison with previously studied pyrene-GCP conjugate (Scheme 1, Py-GCP [8, 10]) revealed several significant improvements of Cy-GCP. Fluorimetric sensing of Py-GCP was based on fluorescence change starting from intrinsic pyrene emission, whereas intrinsically non-fluorescent cyanine gave rise of much stronger fluorescence upon DNA/RNA binding, thus avoiding background fluorescence of non-bound dye. Moreover, Cy-GCP was selective to polynucleotide secondary structure not only by the difference in fluorescence intensity (Table 1:  $QY$ ) but also ICD fingerprint in 300–330 and 450–550 nm regions. Particularly should be stressed high sensitivity of ICD bands (measurable at 200 nM of Cy-GCP).

Moreover, pH-controllable protonation states of Cy-GCP also influence recognition of ds-polynucleotides as well as its complex geometry as confirmed by CD experiments but also self-aggregation of the conjugate.

The combination of cyanine and GCP moiety showed in a preliminary screening to be quite successful for DPP III

inhibition yielding very efficient inhibitor with effect already at 0.2  $\mu\text{M}$  concentration, comparable to the best currently known inhibitor tynorphin [21] but Cy-GCP with the important advantage of being strongly fluorescent upon DPP III binding.

## Experimental

### Synthesis

NMR spectra were recorded on 600 and 300 MHz spectrometers, operating at 150.92 or 75.47 MHz for  $^{13}\text{C}$  and 600.13 or 300.13 MHz for  $^1\text{H}$  nuclei. TMS was used as an internal standard. HRMS analysis was performed on MALDI-TOF mass spectrometer operating in reflectron mode. Mass spectra were acquired by accumulating three spectra after 400 laser shots per spectrum. Calibrant and analyte spectra were obtained in positive ion mode. Calibration type was internal with calibrants produced by matrix ionisation (monomeric, dimeric and trimeric CHCA), with azithromycin and angiotensin II dissolved in  $\alpha$ -cyano-4-hydroxycinnamic acid matrix in the mass range  $m/z = 190.0499\text{--}749.5157$  or 1046.5417. Accurately measured spectra were internally calibrated and elemental analysis was performed on Data Explorer v. 4.9 Software with mass accuracy better than 5 ppm. Samples were prepared by mixing 1  $\text{mm}^3$  of analyte methanol solution with 5  $\text{mm}^3$  of saturated (10  $\text{mg}/\text{cm}^3$ ) solution of  $\alpha$ -cyano-4-hydroxycinnamic acid ( $\alpha$ -CHCA) and internal calibrants (0.1  $\text{mg}/\text{cm}^3$ ) dissolved in 50% acetonitrile/0.1% TFA.

**Cyanine-guanidinocarbonyl-pyrrole conjugate (Cy-GCP, 3,  $\text{C}_{34}\text{H}_{35}\text{ClN}_{10}\text{O}_4\text{S}$ )** Cyanine-amino acid conjugate **1** was prepared by previously described procedure [5] as well as guanidinocarbonyl-pyrrole **2** [22]. Both compounds **1** ( $6.3 \times 10^{-5}$  mol) and **2** ( $1.3 \times 10^{-4}$  mol) were dissolved in acetonitrile ( $2\text{--}3 \text{ cm}^3$ ), and HCTU ( $1.3 \times 10^{-4}$  mol) was added followed by  $\text{Et}_3\text{N}$  ( $2.5 \times 10^{-4}$  mol). The reaction mixture was left stirring at room temperature under argon for 3 days. Boc-protected

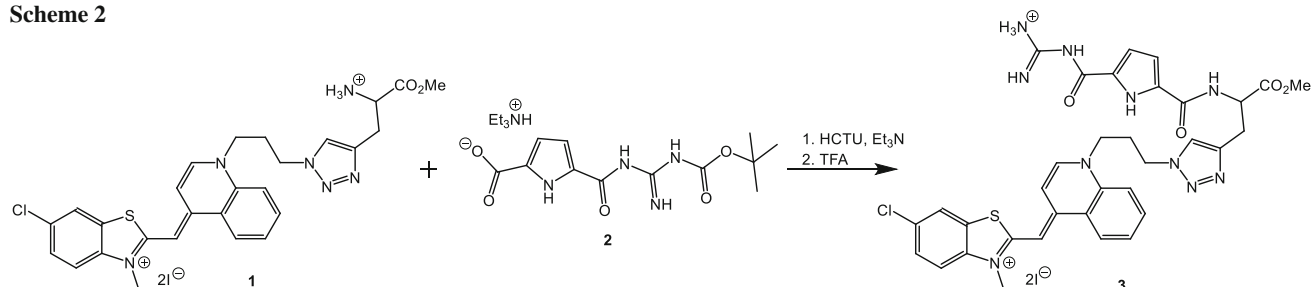
product was deprotected by addition of TFA, the solvent was evaporated and the crude product was recrystallised from methanol-ether mixture and washed with water to give a pure product Cy-GCP in 60% yield as a red solid (Scheme 2).  $^1\text{H}$  NMR (600 MHz,  $\text{DMSO-}d_6$ ):  $\delta = 11.04$  (d,  $J = 69.6$  Hz, 1H, NH), 9.48 (bs, 1H, NH), 8.84–8.74 (m, 1H, Ar), 8.70–8.51 (m, 1H, Ar), 8.24 (dd,  $J = 33.4$ , 16.5 Hz, 4H, Ar), 8.12 (d,  $J = 9.3$  Hz, 1H, Ar), 8.10–7.93 (m, 2H, Ar), 7.82–7.71 (m, 2H, Ar), 7.65 (d,  $J = 6.8$  Hz, 1H, Ar), 7.53–7.26 (m, 1H, Ar), 7.19–6.98 (m, 2H, Ar), 6.93 (s, 1H, CH), 4.92 (t,  $J = 12.3$  Hz, 1H, CH), 4.76 (t,  $J = 5.8$  Hz, 1H, CH), 4.68 (d,  $J = 14.0$  Hz, 1H, CH), 4.58–4.36 (m, 2H,  $\text{CH}_2$ ), 4.00 (s, 3H,  $\text{CH}_3$ ), 3.97–3.86 (m, 2H,  $\text{CH}_2$ ), 3.65 (s, 3H,  $\text{CH}_3$ ), 2.45 (dd,  $J = 26.6$ , 8.4 Hz, 2H,  $\text{CH}_2$ ) ppm;  $^{13}\text{C}$  NMR (151 MHz,  $\text{DMSO-}d_6$ ):  $\delta = 160.0$ , 154.8, 148.9, 144.8, 141.4, 139.6, 137.1, 133.5, 133.4, 128.3, 128.1, 127.4, 126.9, 125.9, 125.6, 124.4, 122.4, 121.4, 118.7, 118.1, 115.5, 115.2, 115.0, 114.1, 109.2, 108.3, 88.5, 78.2, 64.8, 56.0, 51.2, 33.9, 27.4, 15.1 ppm. HRMS (MALDI-TOF/TOF):  $m/z$  calcd for  $\text{C}_{34}\text{H}_{35}\text{ClN}_{10}\text{O}_4\text{S}^{2+}$  ( $[\text{M}]^{2+}$ ) 713.2173, found 713.2181.

### Materials and preparation

All measurements were performed in aqueous buffer solution (pH 7.0,  $I = 0.05$  M, sodium cacodylate/HCl buffer). The UV-Vis spectra were recorded on a Varian Cary 100 Bio spectrometer and fluorescence spectra were recorded on Varian Cary Eclipse fluorimeter in quartz cuvettes (1 cm). Under the experimental conditions used ( $0.1\text{--}1 \times 10^{-6}$  M), the absorbance intensities of Cy-GCP were proportional to their concentrations.

Polynucleotides were purchased as noted: poly dGdC–poly dGdC, poly dAdT–poly dAdT, poly A–poly U, (Sigma), calf thymus ctDNA (Aldrich) and dissolved in sodium cacodylate buffer,  $I = 0.05$  M, pH 7.0. The ctDNA was additionally sonicated and filtered through a 0.45 mm filter [23]. Polynucleotide concentration was determined spectroscopically [24] as the concentration of phosphates.

**Scheme 2**



## Spectroscopic titrations

In fluorimetric experiments, excitation wavelength at  $\lambda_{\text{max}} = 510$  nm was used in order to avoid absorption of excitation light by added polynucleotides. Fluorimetric titrations were performed by adding portions of polynucleotide solution into the solution of the studied compound ( $c = 1 \times 10^{-7}$  M). After mixing polynucleotides with the studied compounds, it was observed in all cases that equilibrium was reached in less than 120 s. Fluorescence spectra were collected at excess of DNA/RNA  $r < 0.1$  [ $r = (\text{compound})/(\text{polynucleotide})$ ] to assure one dominant binding mode. Data were processed by means of non-linear fitting to Scatchard equation [13] (McGhee, von Hippel formalism) [14], which gave values of the ratio of [bound compound]/[polynucleotide] in the range 0.1–0.3, but for easier comparison all  $K_s$  values were re-calculated for the fixed  $n = 0.2$ . Calculated values for  $K_s$  have satisfactory correlation coefficients ( $> 0.99$ ).

CD spectra were recorded on JASCO J-815 spectropolarimeter at room temperature using 1 cm path quartz cuvettes with a scanning speed of 200 nm/min and three averaged repetitions. A buffer background was subtracted from each spectrum. CD experiments were performed by adding portions of compound stock solution into the solution of the polynucleotide ( $c = 2 \times 10^{-5}$  M).

Thermal melting experiments were performed on a Varian Cary 100Bio spectrometer in quartz cuvettes (1 cm). The measurements were done in an aqueous buffer solution at pH 7.0 (sodium cacodylate buffer  $I = 0.05$  M). Thermal melting curves for ds-DNA, ds-RNA and their complexes with Cy-GCP were determined by monitoring the absorption change at 260 nm as a function of temperature [19].  $T_m$  values are the midpoints of the transition curves determined from the maximum of the first derivative and checked graphically by the tangent method. The  $\Delta T_m$  values were calculated subtracting  $T_m$  of the free nucleic acid from  $T_m$  of the complex. Every  $\Delta T_m$  value here reported was the average of at least two measurements. The error in  $\Delta T_m$  is  $\pm 0.5$  °C.

## Peptidase assay

We fluorimetrically monitored the reaction of human DPP III with an artificial substrate Arg<sub>2</sub>-2NA, detecting the release of product 2-naphthylamine ( $\lambda_{\text{exc}} = 332$  nm and  $\lambda_{\text{em}} = 420$  nm), as described by Kumar et al. [25]. The measurements were performed at 25 °C and in 20 mM Tris–HCl buffer pH 7.4. Cy-GCP concentration in the inhibited reaction was 0.2  $\mu$ M. Kinetic parameters were obtained by nonlinear regression analysis of data according

to the Michaelis–Menten model using GraphPad Prism 5 software (GraphPad Software, San Diego, CA, USA, <http://www.graphpad.com>).

**Acknowledgements** This work has been supported by Croatian Science Foundation Projects 7235 and 1477.

## References

- Kuo LC (2011) Fragment-based drug design: tools, practical approaches, and examples. *Methods in enzymology*, vol 493. Academic Press, San Diego
- Gupta RR (2008) Heterocyclic polymethine dyes. Springer, Berlin
- Armitage B (2005) Cyanine dye–DNA interactions: intercalation, groove binding and aggregation. In: DNA binders and related subjects. Springer, Berlin, p 55
- Šmidlehner T, Piantanida I (2017) *Amino Acids* 49:1381
- Šmidlehner T, Kurutos A, Slade J, Belužić R, Ang D, Rodger A, Piantanida I (2018) *Eur J Org Chem*. <https://doi.org/10.1002/ejoc.201701765>
- Tumir LM, Crolatac I, Deligeorgiev T, Vasilev A, Kaloyanova S, Grabar Branilović M, Tomić S, Piantanida I (2012) *Chem Eur J* 18:3859
- Klemm K, Radić Stojković M, Horvat G, Tomišić V, Piantanida I, Schmuck C (2012) *Chem Eur J* 18:1352
- Radić Stojković M, Piotrowski P, Schmuck C, Piantanida I (2015) *Org Biomol Chem* 13:1629
- Langolf S, Machon U, Ehlers M, Langolf S, Sicking W, Schirmeister T, Buchhold C, Gelhaus C, Rosenthal PJ, Schmuck C (2011) *ChemMedChem* 18:1581
- Matić J, Šupljika F, Tir N, Piotrowski P, Schmuck C, Abramić M, Piantanida I, Tomić S (2016) *RSC Adv* 6:83044
- Chen JM, Barrett AJ (2004) Dipeptidyl-peptidase III. In: Barrett AJ, Woessner JF, Rawlings ND (eds) *Handbook of proteolytic enzymes*, 2nd edn. Elsevier, Amsterdam
- Armitage BA (2005) *Top Curr Chem* 253:55
- Scatchard G (1949) *Ann NY Acad Sci* 51:660
- McGhee JD, von Hippel PH (1974) *J Mol Biol* 86:469
- Kubin RF, Fletcher AN (1982) *J Lumin* 27:455
- Cantor CR, Schimmel PR (1980) *Biophysical chemistry*. WH Freeman and Co, San Francisco
- Eriksson M, Norden B (2001) Linear and circular dichroism of drug–nucleic acid complexes. In: Chaires JB, Waring MJ (eds) *Drug–nucleic acid interactions*. *Methods in enzymology*, vol 340. Academic Press, San Diego, p 68
- Šmidlehner T, Piantanida I, Pescitelli G (2018) *Beilstein J Org Chem* 14:84
- Mergny J-L, Lacroix L (2003) *Oligonucleotides* 13:515
- Tumir LM, Piantanida I, Juranovic I, Meic Z, Tomić S, Zinic M (2005) *Chem Commun* 2561
- Yamamoto Y, Hashimoto JI, Shimamura M, Yamaguchi T, Hazato T (2000) *Peptides* 21:503
- Schmuck C (2011) *Synlett* 1798
- Chaires JB, Dattagupta N, Crothers DM (1982) *Biochemistry* 21:3933
- Tumir L-M, Piantanida I, Juranović Cindrić I, Hrenar T, Meić Z, Žinić M (2003) *J Phys Org Chem* 16:891
- Kumar P, Reithofer V, Reisinger M, Wallner S, Pavkov-Keller T, Macheroux P, Gruber K (2016) *Sci Rep* 6:23787